Supporting information

Efficient Yellow and Red Thermally Activated Delayed Fluorescence Materials Based on a Quinoxaline-Derived Electron-Acceptor

Si-Chao Ji [a,b,c], Shanshan Jiang [b,c,e], Tianxiang Zhao [b,c,f], Lingyi Meng [b,c,e], Xu-Lin Chen [b,c,d] * and Can-Zhong Lu [a,b,c,d,f] *

[a] College of Chemistry, Fuzhou University, Fuzhou, Fujian 350108, P.R. China

[b] CAS Key Laboratory of Design and Assembly of Functional Nanostructures, and Fujian Provincial Key Laboratory of Nanomaterials, Fujian Institute of Research on the Structure of Matter, Chinese Academy of Sciences, Fuzhou, Fujian 350002, P.R. China

[c] Xiamen Key Laboratory of Rare Earth Photoelectric Functional Materials, Xiamen Institute of Rare-earth Materials, Haixi Institutes, Chinese Academy of Sciences, Xiamen, Fujian 361021, P.R. China

[d] Fujian Science & Technology Innovation Laboratory for Optoelectronic Information of China, Fuzhou, Fujian 350108, P. R. China

[e] Jiangxi Provincial Key Laboratory of Functional Molecular Materials Chemistry, Department of Materials, Metallurgy and Chemistry, Jiangxi University of Science and Technology, Ganzhou 341000, P. R. China

[f] University of Chinese Academy of Sciences, P.R. China

* Corresponding authors.

Can-Zhong Lu, E-mail: czlu@fjirsm.ac.cn

Xu-Lin Chen, E-mail: xlchem@fjirsm.ac.cn

Table of Contents

1. Synthesis of Materials

1, 2-bis (4-(9, 9-dimethylacridin-10(9H)-yl) phenyl) ethane-1, 2-dione (DDMAC-BZ)

To a solution of 4, 4'-Dibromobenzil (1.1 g, 3 mmol), 9,9-dimethyl-9,10-dihydro-acridine (1.38 g, 6.6 mmol), cesium carbonate (3.91 g, 12.00 mmol), and tri-tert-butylphosphonium tetrafluoroborate (131 mg, 0.45 mmol) in dry toluene (60 mL), palladium (II) acetate (34 mg, 0.15 mmol) was added, and then the mixture was refluxed at 110°C for 12h under a nitrogen atmosphere. After cooling, the mixture was extracted with brine and CH_2Cl_2. The collected organic phase was dried over anhydrous Na_2SO_4 and concentrated by rotary evaporation. The crude product was purified by column chromatography on silica gel to give an orange powder (1.2 g, 64%). ^{1}H NMR (500 MHz, $CDCl_3$) δ 8.28 (d, *J* = 8.6 Hz, 4H), 7.57 (d, *J* = 8.5 Hz, 4H), 7.52 (d, *J* = 1.9 Hz, 2H), 7.50 (d, *J* = 1.9 Hz, 2H), 7.06 (ddd, *J* = 9.3, 7.5, 1.7 Hz, 8H), 6.53 (d, *J* = 1.6 Hz, 2H), 6.51 (d, *J* = 1.6 Hz, 2H), 1.69 (s, 12H).

1, 2-bis (4-(10H-phenoxazin-10-yl) phenyl) ethane-1, 2-dione (DPXZ-BZ)

The synthesis process was referred to the reported literature.[1]

10, 10'-((6, 7-dibromoquinoxaline-2, 3-diyl) bis (4, 1-phenylene)) bis (9, 9-dimethyl-9, 10-dihydroacridine) (BrQP-DDMAC)

DDMAC-BZ (937.2 mg, 1.5 mmol) and 4, 5-Dibromobenzene-1, 2-diamine (398.9 mg, 1.5 mmol) were added into a two-necked round-bottomed flask containing 25 mL dry 1-Butanol. The mixture was refluxed at 120°C for 12h under a nitrogen atmosphere. When the reaction completed, the reaction mixture was extracted with brine and CH_2Cl_2, and dried over anhydrous Na_2SO_4, and concentrated in vacuum. The crude product was purified by column chromatography on silica gel to give the product as a yellowish green solid (0.94 g, 73%). ^{1}H NMR (500 MHz, $CDCl_3$) δ 8.62 (s, 1H), 8.20 (d, *J* = 8.4 Hz, 1H), 7.86 (d, *J* = 8.4 Hz, 3H), 7.57 (d, *J* = 8.4 Hz, 1H), 7.52 (dd, *J* = 7.6, 1.7 Hz, 1H), 7.48 (dd, *J* = 7.6, 1.7 Hz, 3H), 7.44 (d, *J* = 8.4 Hz, 3H), 7.03 (ddd, *J* = 14.7, 7.7, 1.5 Hz, 2H), 6.95 – 6.84 (m, 7H), 6.40 (dd, *J* = 8.0, 1.4 Hz, 1H), 6.35 (dd, *J* = 8.1, 1.4 Hz, 3H), 1.72 (d, *J* = 11.3 Hz, 12H).

10, 10'-((6, 7-dibromoquinoxaline-2, 3-diyl) bis (4, 1-phenylene)) bis (10H-

phenoxazine) (BrQP-DPXZ)

It was prepared by the same procedure with BrQP-DDMAC excepting using the DPXZ-BZ (860 mg, 1.5 mmol). And get DPXZ-BZ is an orange solid (0.84 g, 70 %). ^{1}H NMR (500 MHz, $CDCl_3$) δ 8.57 (s, 2H), 7.77 (d, *J* = 8.4 Hz, 4H), 7.40 (d, *J* = 8.5 Hz, 4H), 6.70 (dd, *J* = 7.9, 1.5 Hz, 4H), 6.64 (td, *J* = 7.6, 1.4 Hz, 4H), 6.54 (d, *J* = 1.5 Hz, 1H), 6.52 (d, *J* = 1.5 Hz, 2H), 6.51 (d, *J* = 1.5 Hz, 1H), 5.95 (dd, *J* = 7.9, 1.5 Hz, 4H).

4, 4'-(2, 3-bis (4-(9, 9-dimethylacridin-10(9H)-yl) phenyl) quinoxaline-6, 7-diyl) dibenzonitrile (DMAC-QCN)

A two-necked round-bottomed flask was charged with BrQP-DDMAC (854.7 mg, 1 mmol), 4-Cyanophenylboronic acid (441 mg, 3 mmol), $Pd(PPh_3)_4$ (57.8 mg, 0.05 mmol), K_2CO_3 (414.6 mg, 3 mmol) and THF/H_2O solution (15 ml/3 ml). The flask was then evacuated and purged with nitrogen gas for three times and the mixture was refluxed at 70°C for 12h under a nitrogen atmosphere. After cooled to room temperature, the solution was extracted several times with ethyl acetate and brine, and dried over anhydrous Na_2SO_4, and concentrated in vacuum. Then the crude product was purified via column chromatography on silica gel to give the product as a yellowish green solid (0.61 g, 68%). ^{1}H NMR (500 MHz, $CDCl_3$) δ 8.37 (s, 2H), 7.89 (d, *J* = 8.3 Hz, 4H), 7.66 (d, *J* = 8.3 Hz, 4H), 7.48 – 7.38 (m, 12H), 6.93 – 6.83 (m, 8H), 6.34 (dd, *J* = 8.1, 1.4 Hz, 4H), 1.69 (s, 12H). ^{13}C NMR (126 MHz, $CDCl_3$) δ 154.37, 144.15, 142.60, 141.21, 140.86, 140.61, 138.26, 132.44, 132.34, 131.50, 131.24, 130.52, 130.37, 126.52, 125.19, 120.93, 118.35, 114.02, 111.91, 36.05, 30.91. Anal. calcd. for $C_{64}H_{46}N_6$: C, 85.50; H, 5.16; N, 9.35. Found: C, 85.42; H, 5.12; N, 9.33.

4, 4'-(2, 3-bis (4-(10H-phenoxazin-10-yl) phenyl) quinoxaline-6, 7-diyl) dibenzonitrile (PXZ-QCN)

It was prepared by the same procedure with DMAC-QCN excepting using the BrQP-DPXZ (802.5 mg, 1 mmol). And get PXZ-QCN is an orange solid (0.65 g, 77 %). ^{1}H NMR (500 MHz, $CDCl_3$) δ 8.34 (s, 2H), 7.82 (d, *J* = 8.4 Hz, 4H), 7.65 (d, *J* = 8.4 Hz, 4H), 7.43 (d, *J* = 8.4 Hz, 4H), 7.38 (d, *J* = 8.4 Hz, 4H), 6.70 (dd, *J* = 7.9, 1.5 Hz, 4H),

6.64 (td, J = 7.6, 1.4 Hz, 4H), 6.53 (td, J = 7.7, 1.5 Hz, 4H), 5.96 (dd, J = 8.0, 1.4 Hz, 4H). ^{13}C NMR (126 MHz, $CDCl_3$) δ 153.98, 144.04, 143.97, 141.40, 140.72, 140.43, 138.35, 133.83, 132.61, 132.35, 131.13, 131.05, 130.50, 123.41, 121.75, 118.31, 115.69, 113.15, 111.97. Anal. calcd. For $C_{58}H_{34}N_6O_2$: C, 82.25; H, 4.05; N, 9.92. Found: C, 82.29; H, 4.07; N, 9.97.

2. NMR Spectra

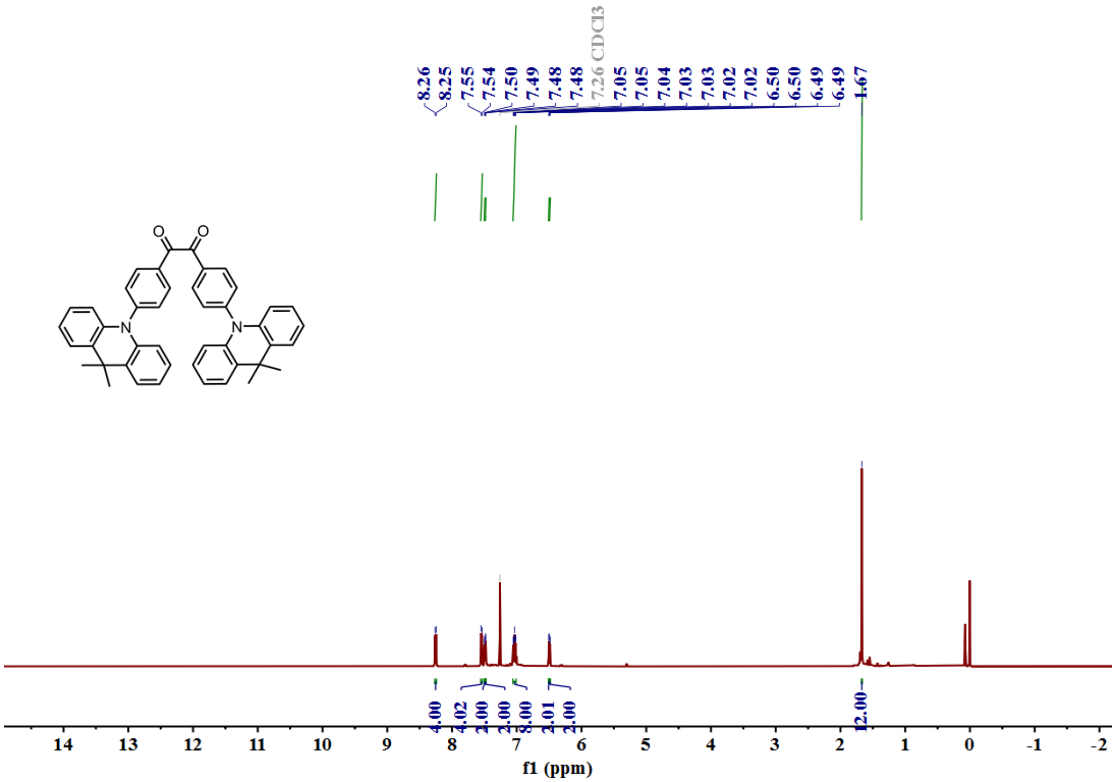

Figure S1. ^{1}H-NMR spectrum of DDMAC-BZ (500 MHz, $CDCl_3$).

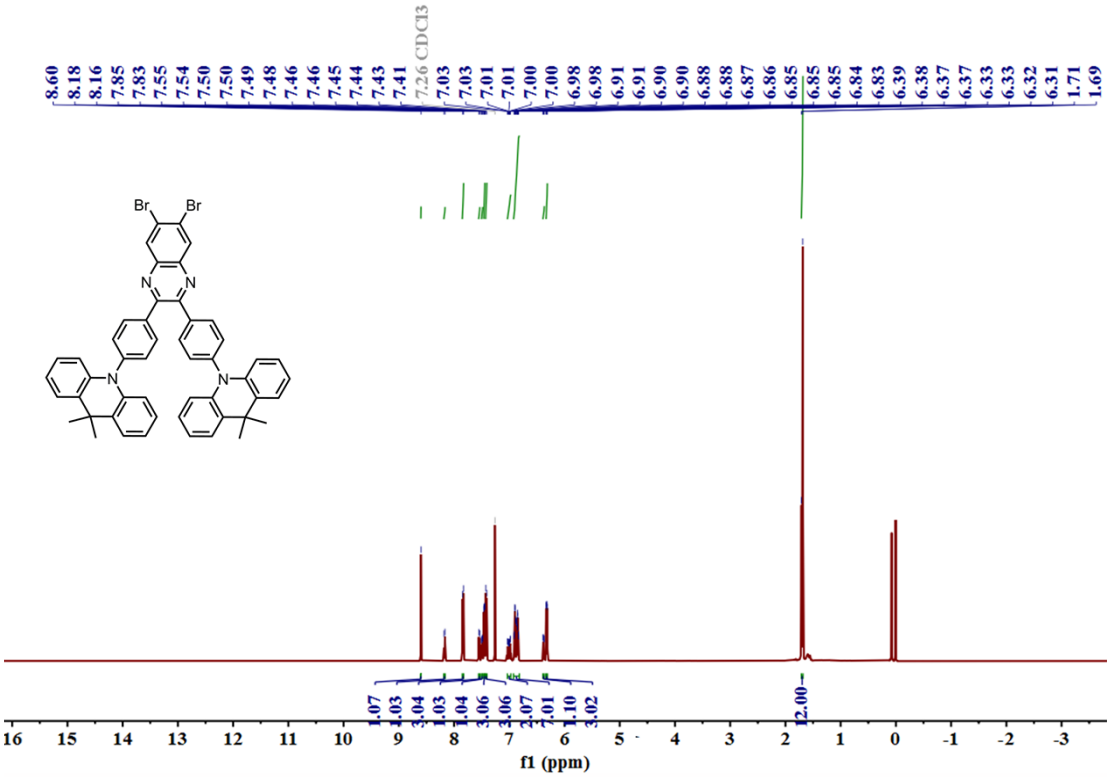

Figure S2. ^{1}H-NMR spectrum of BrQP-DDMAC (500 MHz, $CDCl_3$).

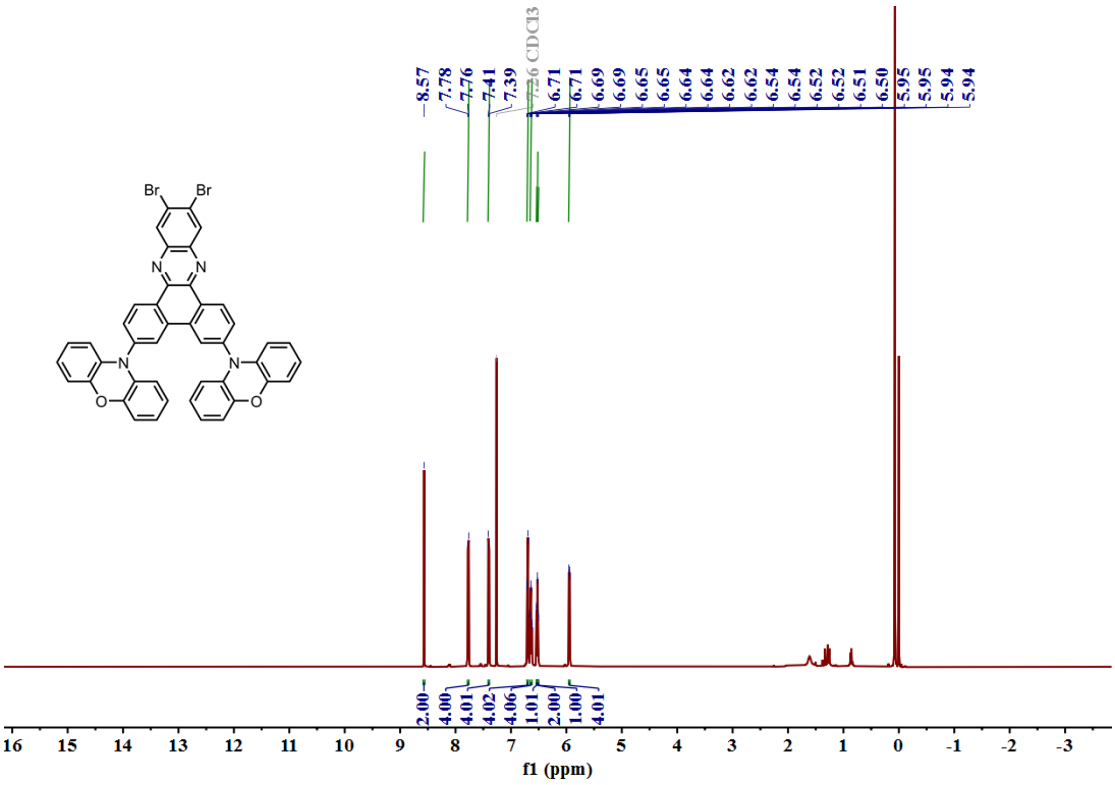

Figure S3. ^{1}H-NMR spectrum of BrQP-DPXZ (500 MHz, $CDCl_3$).

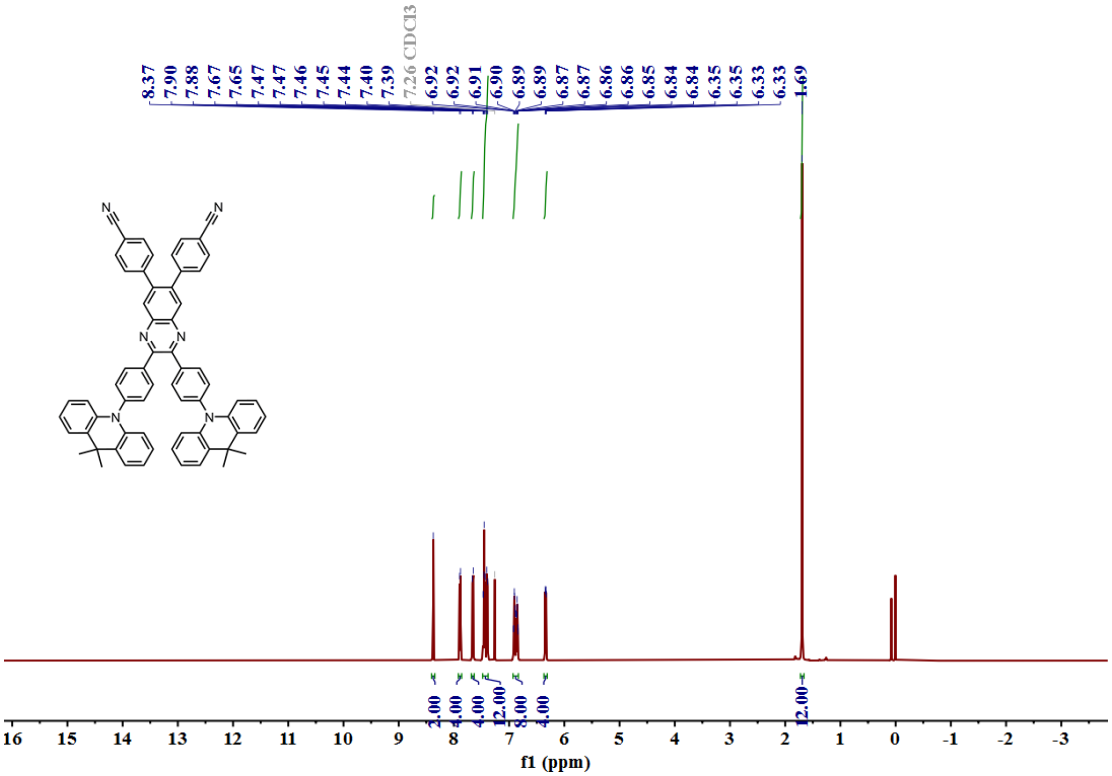

Figure S4. ^{1}H-NMR spectrum of DMAC-QCN (500 MHz, $CDCl_3$).

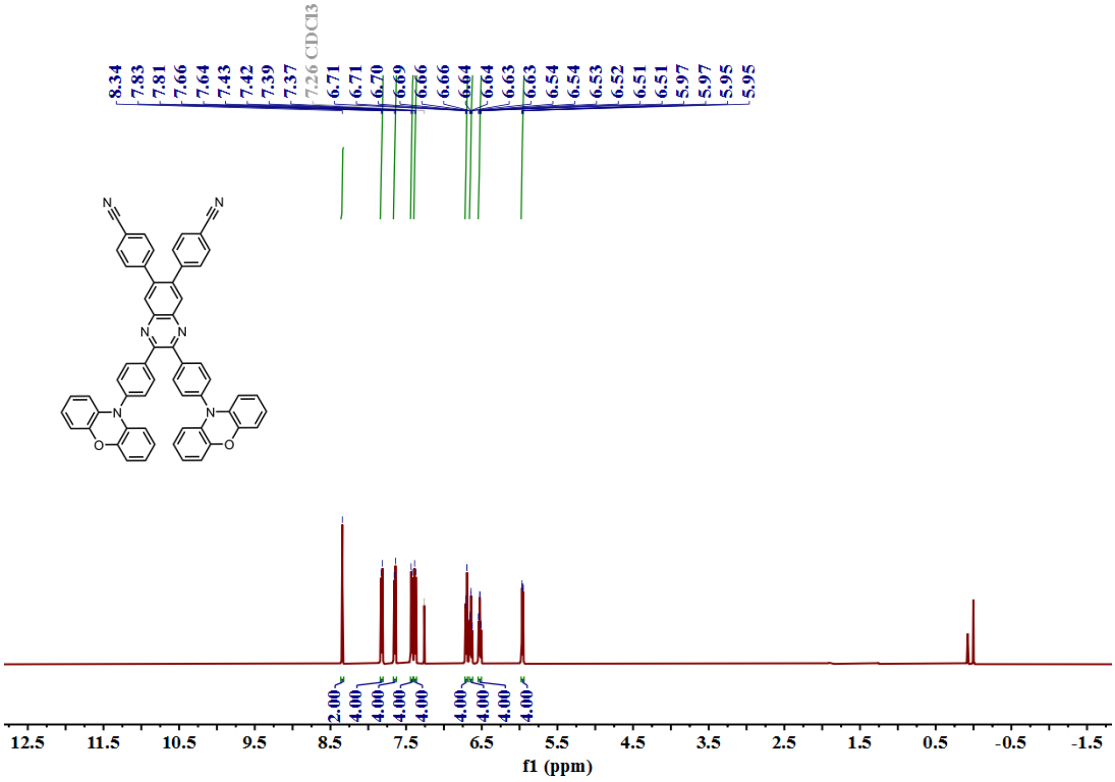

Figure S5. ^{1}H-NMR spectrum of PXZ-QCN (500 MHz, $CDCl_3$).

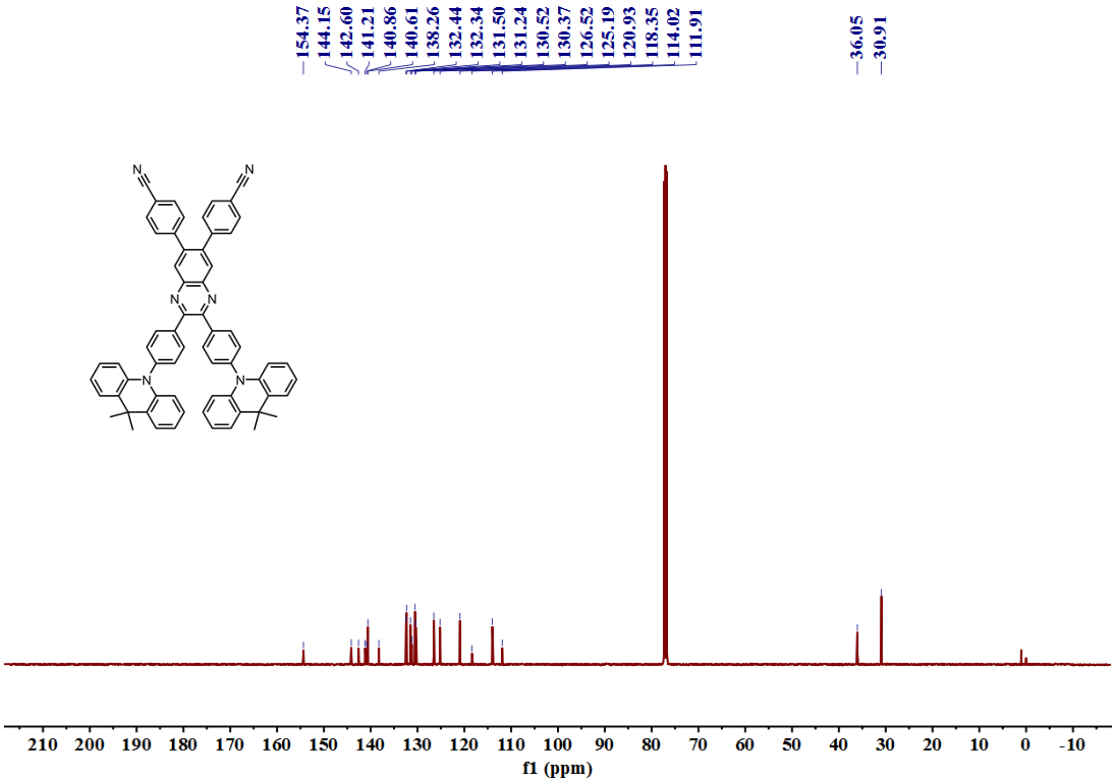

Figure S6. ^{13}C-NMR spectrum of DMAC-QCN (500 MHz, $CDCl_3$).

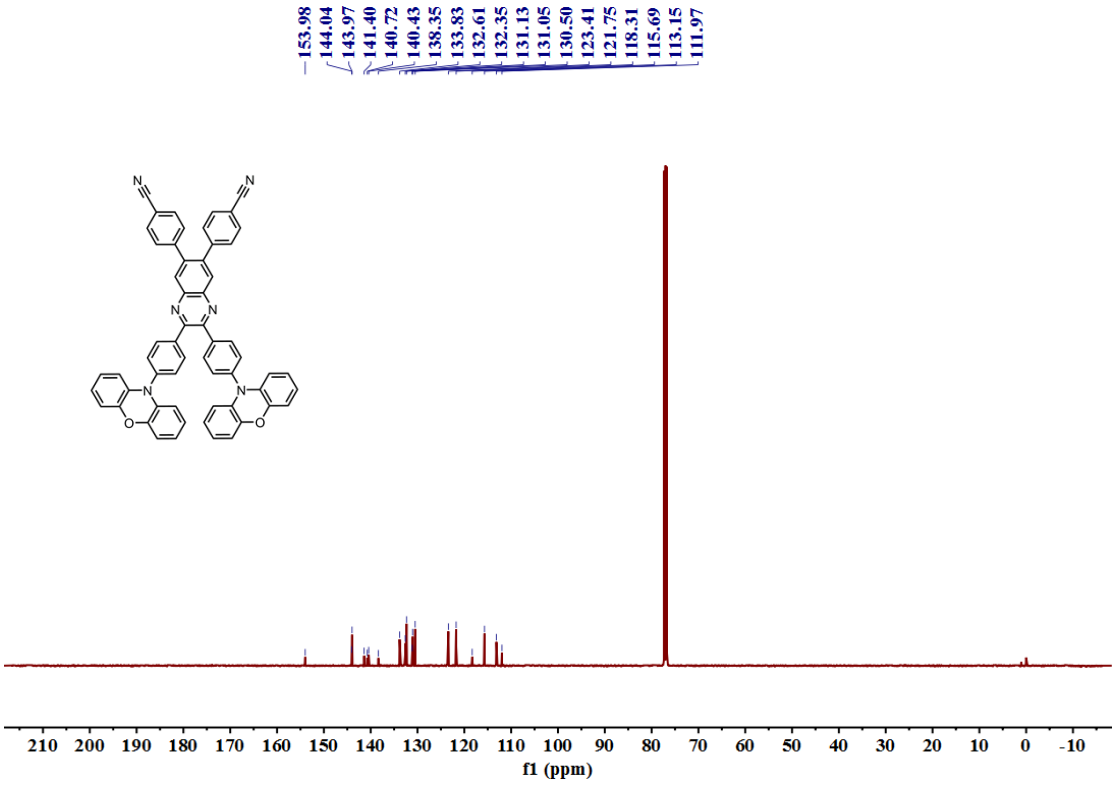

Figure S7. ^{13}C-NMR spectrum of PXZ-QCN (500 MHz, $CDCl_3$).

3. X-ray Crystallographic Analysis

Table S1. Crystal data and structure refinements for DMAC-QCN and PXZ-QCN.

Compounds	DMAC-QCN	PXZ-QCN
Empirical formula	$C_{64}H_{46}N_6$	$C_{58}H_{34}N_6O_2$
Formula weight	899.07	846.91
Temperature/K	200.00	200.00
Crystal system	triclinic	triclinic
Space group	P-1	P-1
a/Å	10.5869(4)	11.0106(5)
b/Å	14.2196(6)	15.1674(8)
c/Å	16.8639(7)	15.2817(9)
α/°	87.049(2)	77.222(2)
β/°	82.503(2)	73.086(2)
γ/°	74.066(2)	74.851(2)
Volume/Å^3	2419.98(17)	2327.5(2)
Z	2	2
ρ_{calc}g/cm^3	1.234	1.208
μ/mm^{-1}	0.073	0.075
F(000)	944.0	880.0
Crystal size/mm^3	0.15 × 0.1 × 0.06	0.16 × 0.04 × 0.03
Radiation	MoKα (λ = 0.71073)	MoKα (λ = 0.71073)
2Θ range for data collection/°	3.818 to 55.034	5.32 to 49.994
Index ranges	$-13 \leq h \leq 13$, $-18 \leq k \leq 18$, $-21 \leq l \leq 21$	$-13 \leq h \leq 13$, $-18 \leq k \leq 18$, $-18 \leq l \leq 18$
Reflections collected	107112	90423
Independent reflections	11104 [R_{int} = 0.1571, R_{sigma} = 0.0773]	8170 [R_{int} = 0.1268, R_{sigma} = 0.0538]
Data/restraints/parameters	11104/0/635	8170/0/571
Goodness-of-fit on F^2	1.016	1.119
Final R indexes [I>=2σ (I)]	R_1 = 0.0614, wR_2 =	R_1 = 0.0654, wR_2 =

	0.1260	0.1668
Final R indexes [all data]	R_1 = 0.1423, wR_2 = 0.1627	R_1 = 0.1177, wR_2 = 0.1862
Largest diff. peak/hole / e $Å^{-3}$	0.20/-0.26	0.80/-0.44

Table S2. Bond Lengths for DMAC-QCN.

Atom	Atom	Length/Å	Atom	Atom	Length/Å
N1	C4	1.412(3)	C22	C23	1.381(4)
N1	C5	1.442(3)	C23	C24	1.489(3)
N1	C51	1.412(3)	C23	C63	1.389(3)
N2	C14	1.438(3)	C24	C25	1.436(3)
N2	C15	1.421(3)	C24	C42	1.371(3)
N2	C33	1.411(3)	C25	C26	1.367(3)
N3	C19	1.146(3)	C25	C56	1.495(3)
N4	C10	1.320(3)	C26	C27	1.410(3)
N4	C27	1.370(3)	C27	C41	1.402(3)
N5	C9	1.322(3)	C28	C29	1.399(4)
N5	C41	1.363(3)	C29	C30	1.520(4)
N6	C60	1.146(3)	C30	C31	1.553(4)
C1	C2	1.547(4)	C30	C32	1.515(4)
C2	C3	1.525(3)	C30	C38	1.533(3)
C2	C49	1.541(3)	C32	C33	1.404(3)
C2	C50	1.527(3)	C32	C37	1.389(4)
C3	C4	1.396(3)	C33	C34	1.395(4)
C3	C45	1.390(3)	C34	C35	1.385(4)
C4	C48	1.397(3)	C35	C36	1.385(4)
C5	C6	1.387(3)	C36	C37	1.380(4)
C5	C43	1.377(3)	C39	C40	1.385(3)
C6	C7	1.381(3)	C41	C42	1.409(3)

C7	C8	1.399(3)	C43	C44	1.386(3)
C8	C9	1.490(3)	C45	C46	1.381(4)
C8	C44	1.398(3)	C46	C47	1.375(4)
C9	C10	1.438(3)	C47	C48	1.381(3)
C10	C11	1.491(3)	C50	C51	1.401(3)
C11	C12	1.390(3)	C50	C55	1.393(3)
C11	C40	1.390(3)	C51	C52	1.387(3)
C12	C13	1.385(3)	C52	C53	1.376(3)
C13	C14	1.388(3)	C53	C54	1.375(4)
C14	C39	1.384(3)	C54	C55	1.380(4)
C15	C16	1.392(3)	C56	C57	1.389(3)
C15	C29	1.397(3)	C56	C62	1.392(3)
C16	C17	1.383(3)	C57	C58	1.383(3)
C17	C18	1.378(4)	C58	C59	1.385(4)
C18	C28	1.377(4)	C59	C60	1.442(4)
C19	C20	1.442(4)	C59	C61	1.381(4)
C20	C21	1.384(4)	C61	C62	1.383(3)
C20	C64	1.379(4)	C63	C64	1.380(3)
C21	C22	1.389(4)			

Table S3. Bond Angles for DMAC-QCN.

Atom	Atom	Atom	Angle/°	Atom	Atom	Atom	Angle/°
C4	N1	C5	117.60(17)	C26	C25	C24	119.6(2)
C51	N1	C4	120.33(18)	C26	C25	C56	120.3(2)
C51	N1	C5	120.89(18)	C25	C26	C27	121.1(2)
C15	N2	C14	119.25(19)	N4	C27	C26	119.4(2)
C33	N2	C14	117.29(19)	N4	C27	C41	121.04(19)
C33	N2	C15	118.60(19)	C41	C27	C26	119.50(19)
C10	N4	C27	117.23(18)	C18	C28	C29	122.4(3)
C9	N5	C41	117.69(18)	C15	C29	C28	117.7(3)

C3	C2	C1	107.7(2)	C15	C29	C30	118.3(2)
C3	C2	C49	110.9(2)	C28	C29	C30	123.8(2)
C3	C2	C50	109.65(19)	C29	C30	C31	107.7(2)
C49	C2	C1	108.7(2)	C29	C30	C38	112.3(2)
C50	C2	C1	108.5(2)	C32	C30	C29	107.5(2)
C50	C2	C49	111.3(2)	C32	C30	C31	108.6(2)
C4	C3	C2	120.9(2)	C32	C30	C38	112.8(3)
C45	C3	C2	121.1(2)	C38	C30	C31	107.8(2)
C45	C3	C4	117.6(2)	C33	C32	C30	118.6(2)
C3	C4	N1	119.53(19)	C37	C32	C30	123.7(3)
C3	C4	C48	120.3(2)	C37	C32	C33	117.5(3)
C48	C4	N1	120.1(2)	C32	C33	N2	118.5(2)
C6	C5	N1	118.6(2)	C34	C33	N2	121.1(2)
C43	C5	N1	121.3(2)	C34	C33	C32	120.4(2)
C43	C5	C6	119.8(2)	C35	C34	C33	120.6(3)
C7	C6	C5	119.9(2)	C34	C35	C36	119.2(3)
C6	C7	C8	121.0(2)	C37	C36	C35	120.0(3)
C7	C8	C9	118.11(19)	C36	C37	C32	122.1(3)
C44	C8	C7	118.2(2)	C14	C39	C40	120.2(2)
C44	C8	C9	123.4(2)	C39	C40	C11	120.5(2)
N5	C9	C8	113.93(19)	N5	C41	C27	121.20(19)
N5	C9	C10	121.07(19)	N5	C41	C42	119.6(2)
C10	C9	C8	124.98(18)	C27	C41	C42	119.1(2)
N4	C10	C9	121.77(19)	C24	C42	C41	121.4(2)
N4	C10	C11	115.23(19)	C5	C43	C44	120.7(2)
C9	C10	C11	122.99(18)	C43	C44	C8	120.3(2)
C12	C11	C10	120.26(19)	C46	C45	C3	122.2(2)
C40	C11	C10	120.8(2)	C47	C46	C45	119.6(2)
C40	C11	C12	119.0(2)	C46	C47	C48	119.9(2)

C13	C12	C11	120.7(2)	C47	C48	C4	120.3(2)
C12	C13	C14	119.8(2)	C51	C50	C2	120.9(2)
C13	C14	N2	118.8(2)	C55	C50	C2	121.7(2)
C39	C14	N2	121.31(19)	C55	C50	C51	117.2(2)
C39	C14	C13	119.9(2)	C50	C51	N1	119.2(2)
C16	C15	N2	121.8(2)	C52	C51	N1	120.2(2)
C16	C15	C29	119.7(2)	C52	C51	C50	120.6(2)
C29	C15	N2	118.5(2)	C53	C52	C51	120.7(2)
C17	C16	C15	120.8(2)	C54	C53	C52	119.5(2)
C18	C17	C16	120.0(3)	C53	C54	C55	120.1(2)
C28	C18	C17	119.0(3)	C54	C55	C50	121.9(2)
N3	C19	C20	176.2(3)	C57	C56	C25	118.9(2)
C21	C20	C19	120.5(3)	C57	C56	C62	118.7(2)
C64	C20	C19	118.6(3)	C62	C56	C25	122.3(2)
C64	C20	C21	120.8(2)	C58	C57	C56	120.9(2)
C20	C21	C22	119.2(3)	C57	C58	C59	119.5(3)
C23	C22	C21	120.6(3)	C58	C59	C60	118.5(3)
C22	C23	C24	120.6(2)	C61	C59	C58	120.4(2)
C22	C23	C63	119.1(2)	C61	C59	C60	121.1(3)
C63	C23	C24	120.3(2)	N6	C60	C59	178.2(4)
C25	C24	C23	120.4(2)	C59	C61	C62	119.7(2)
C42	C24	C23	120.2(2)	C61	C62	C56	120.7(2)
C42	C24	C25	119.3(2)	C64	C63	C23	120.9(3)
C24	C25	C56	119.96(19)	C20	C64	C63	119.3(3)

Table S4. Bond Lengths for PXZ-QCN.

Atom	Atom	Length/Å	Atom	Atom	Length/Å
O1	C18	1.390(3)	C19	C57	1.364(4)
O1	C19	1.387(3)	C20	C54	1.378(4)
O2	C31	1.392(4)	C21	C22	1.393(4)

O2	C32	1.379(3)	C21	C39	1.388(4)
N1	C1	1.148(4)	C22	C23	1.384(4)
C2	C4	1.330(4)	C23	C24	1.382(4)
C2	C5	1.560(4)	C24	N25	1.440(3)
C2	C44	1.368(4)	C24	C38	1.379(4)
N3	C7	1.377(3)	N25	C26	1.404(4)
N3	C8	1.315(3)	N25	C37	1.401(3)
N4	C13	1.434(3)	C26	C27	1.388(4)
N4	C14	1.405(3)	C26	C31	1.401(4)
N4	C20	1.391(3)	C27	C28	1.391(4)
N5	C49	1.147(3)	C28	C29	1.390(5)
N6	C9	1.324(3)	C29	C30	1.380(5)
N6	C40	1.362(3)	C30	C31	1.366(4)
C1	C25	1.437(4)	C32	C33	1.372(4)
C25	C3	1.399(4)	C32	C37	1.392(4)
C25	C43	1.380(4)	C33	C34	1.381(4)
C3	C4	1.386(4)	C34	C35	1.372(4)
C5	C6	1.371(3)	C35	C36	1.388(4)
C5	C42	1.444(3)	C36	C37	1.390(4)
C6	C7	1.408(4)	C38	C39	1.377(4)
C7	C40	1.399(3)	C40	C41	1.410(3)
C8	C9	1.438(3)	C41	C42	1.373(4)
C8	C21	1.484(3)	C42	C45	1.513(3)
C9	C10	1.490(4)	C43	C44	1.379(4)
C10	C11	1.399(4)	C45	C46	1.383(4)
C10	C52	1.399(3)	C45	C51	1.373(4)
C11	C12	1.381(4)	C46	C47	1.383(4)
C12	C13	1.377(4)	C47	C48	1.385(4)
C13	C53	1.384(4)	C48	C49	1.450(4)

C14	C15	1.377(4)	C48	C50	1.386(4)
C14	C18	1.386(4)	C50	C51	1.379(4)
C15	C16	1.384(4)	C52	C53	1.381(4)
C16	C17	1.387(5)	C54	C55	1.376(5)
C17	C58	1.376(5)	C55	C56	1.377(5)
C18	C58	1.366(4)	C56	C57	1.378(5)
C19	C20	1.392(4)			

Table S5. Bond Angles for PXZ-QCN.

Atom	Atom	Atom	Angle/°	Atom	Atom	Atom	Angle/°
C19	O1	C18	117.8(2)	C24	C23	C22	120.1(3)
C32	O2	C31	117.6(2)	C23	C24	N25	119.0(3)
C4	C2	C5	118.5(2)	C38	C24	C23	119.8(3)
C4	C2	C44	123.2(3)	C38	C24	N25	121.1(3)
C44	C2	C5	118.1(3)	C26	N25	C24	121.3(2)
C8	N3	C7	117.2(2)	C37	N25	C24	119.3(2)
C14	N4	C13	119.8(2)	C37	N25	C26	119.0(2)
C20	N4	C13	120.3(2)	C27	C26	N25	124.1(3)
C20	N4	C14	118.8(2)	C27	C26	C31	117.4(3)
C9	N6	C40	117.1(2)	C31	C26	N25	118.5(3)
N1	C1	C25	178.6(4)	C26	C27	C28	121.4(3)
C3	C25	C1	120.6(3)	C27	C28	C29	119.4(3)
C43	C25	C1	119.9(3)	C30	C29	C28	120.0(3)
C43	C25	C3	119.5(3)	C31	C30	C29	120.0(3)
C4	C3	C25	118.9(3)	O2	C31	C26	121.6(3)
C2	C4	C3	119.8(3)	C30	C31	O2	116.5(3)
C6	C5	C2	119.3(2)	C30	C31	C26	121.9(3)
C6	C5	C42	118.6(2)	O2	C32	C37	121.5(3)
C42	C5	C2	122.1(2)	C33	C32	O2	117.9(3)
C5	C6	C7	122.1(2)	C33	C32	C37	120.6(3)

N3	C7	C6	120.0(2)	C32	C33	C34	120.9(3)
N3	C7	C40	120.7(2)	C35	C34	C33	119.2(3)
C40	C7	C6	119.2(2)	C34	C35	C36	120.3(3)
N3	C8	C9	121.8(2)	C37	C36	C35	120.7(3)
N3	C8	C21	116.2(2)	C32	C37	N25	119.4(3)
C9	C8	C21	121.9(2)	C36	C37	N25	122.3(2)
N6	C9	C8	121.3(2)	C36	C37	C32	118.2(3)
N6	C9	C10	115.9(2)	C39	C38	C24	120.0(3)
C8	C9	C10	122.6(2)	C38	C39	C21	121.0(3)
C11	C10	C9	118.3(2)	N6	C40	C7	121.7(2)
C52	C10	C9	123.8(2)	N6	C40	C41	119.0(2)
C52	C10	C11	117.9(3)	C7	C40	C41	119.2(2)
C12	C11	C10	121.1(3)	C42	C41	C40	121.4(2)
C13	C12	C11	120.0(3)	C5	C42	C45	122.2(2)
C12	C13	N4	120.1(3)	C41	C42	C5	119.4(2)
C12	C13	C53	120.0(3)	C41	C42	C45	118.3(2)
C53	C13	N4	119.9(2)	C44	C43	C25	120.5(3)
C15	C14	N4	123.0(3)	C2	C44	C43	118.1(3)
C15	C14	C18	117.5(3)	C46	C45	C42	119.5(2)
C18	C14	N4	119.6(3)	C51	C45	C42	120.9(2)
C14	C15	C16	120.8(3)	C51	C45	C46	119.7(2)
C15	C16	C17	120.2(3)	C47	C46	C45	120.2(3)
C58	C17	C16	119.6(3)	C46	C47	C48	119.5(3)
C14	C18	O1	121.4(2)	C47	C48	C49	120.0(3)
C58	C18	O1	115.9(3)	C47	C48	C50	120.5(3)
C58	C18	C14	122.7(3)	C50	C48	C49	119.4(3)
O1	C19	C20	121.1(3)	N5	C49	C48	179.6(4)
C57	C19	O1	116.5(3)	C51	C50	C48	119.0(3)
C57	C19	C20	122.3(3)	C45	C51	C50	121.1(3)

N4	C20	C19	120.0(2)	C53	C52	C10	120.7(3)
C54	C20	N4	122.6(3)	C52	C53	C13	120.2(3)
C54	C20	C19	117.4(3)	C55	C54	C20	120.9(3)
C22	C21	C8	120.4(2)	C54	C55	C56	120.5(3)
C39	C21	C8	121.2(2)	C55	C56	C57	119.6(4)
C39	C21	C22	118.5(2)	C19	C57	C56	119.3(3)
C23	C22	C21	120.4(3)	C18	C58	C17	119.2(3)

4. Thermal and Electrochemical Properties

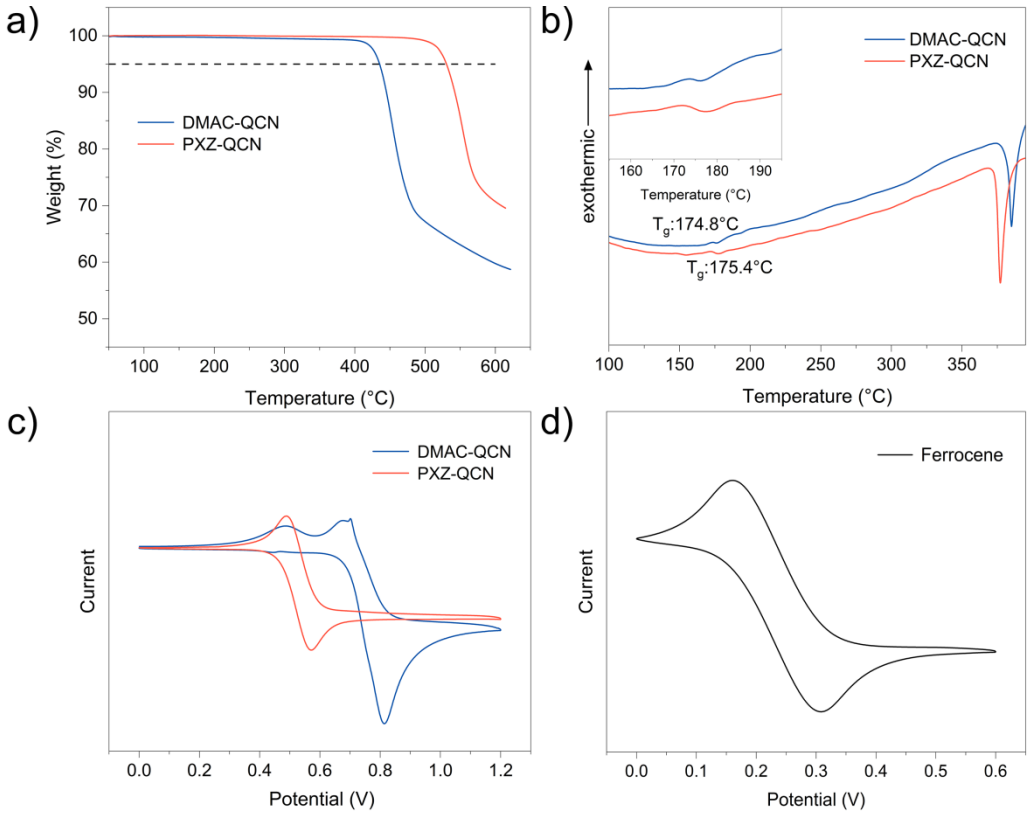

Figure S8. a) Thermal gravimetric analysis (TGA) traces of DMAC-QCN and PXZ-QCN. b) Differential scanning calorimetry (DSC) curves of DMAC-QCN and PXZ-QCN. Inset: magnified image of the selected region. c) Cyclic Voltammograms for the oxidation of DMAC-QCN and PXZ-QCN. d) Oxidation behaviours of Ferrocene

The CV measurements were carried out in anhydrous and nitrogen-saturated dichloromethane (DCM) solutions with 0.1 M n-Bu_4NPF_6 and 1.0 mM investigated compounds. Using glassy carbon electrode as working electrode, platinum wire as auxiliary electrode, porous glass wick $Ag/AgNO_3$ as reference electrode and

ferrocene/ferrocenium as the internal standard. The HOMO energy level was calculated from the onset potential of oxidation by cyclic voltammetry.

[HOMO = - (4.8- $E_{1/2(Fc/Fc+)}$ + E_{onset})]

The LUMO energy level was determined from the difference between the HOMO levels and optical band gap (E_g) estimated from the onset of the UV-Vis absorption band.

$E_g = 1241 / \lambda_{onset}$ [LUMO = HOMO + E_g]

Table S6. Summary of thermal and electrochemical properties of DMAC-QCN and PXZ-QCN.

Compound	T_d [a] (°C)	T_g [b] (°C)	HOMO [c] (eV)	LUMO [d] (eV)	E_g [e] (eV)
DMAC-QCN	435.0	174.8	-5.24	-2.62	2.62
PXZ-QCN	530.0	175.4	-5.02	-2.58	2.44

[a] Decomposition temperature corresponding to 5% weight loss. [b] Glass transition temperature. [c] Obtained from the CV curves. [d] Calculated from the E_g and HOMO levels. [e] Optical energy gaps (E_g) were determined from the UV-Vis absorption spectra.

5. Photophysical Properties

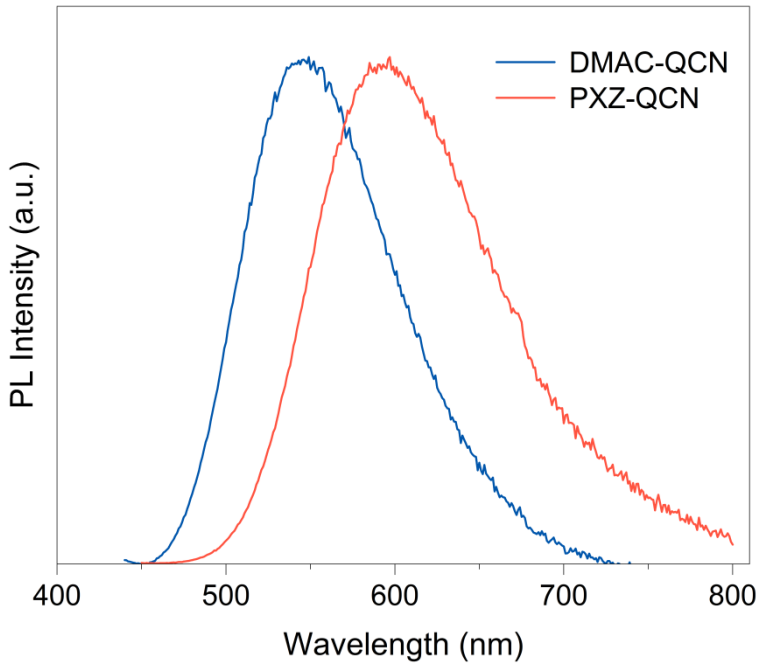

Figure S9. Normalized PL spectra of DMAC-QCN and PXZ-QCN in 20 wt% doped CBP film at 298K.

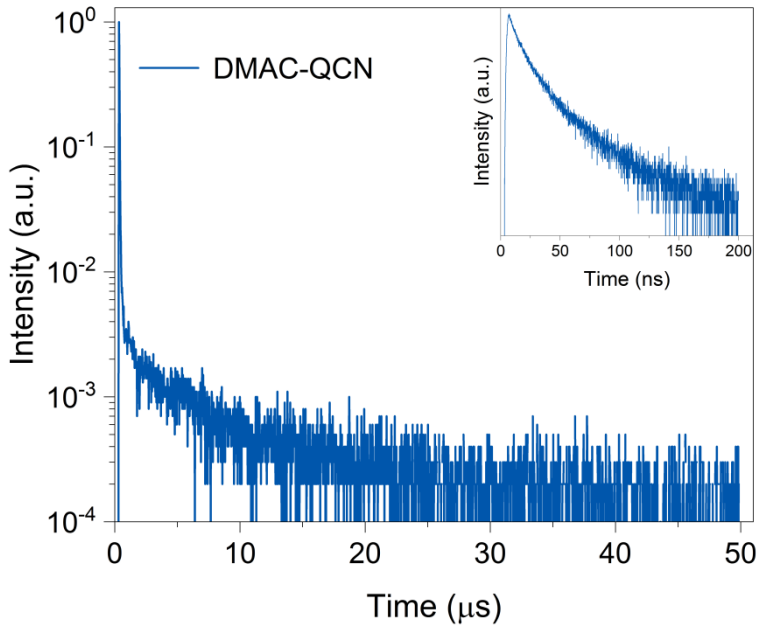

Figure S10. Transient PL decay curve of DMAC-QCN in 20 wt% doped CBP film at 298K.

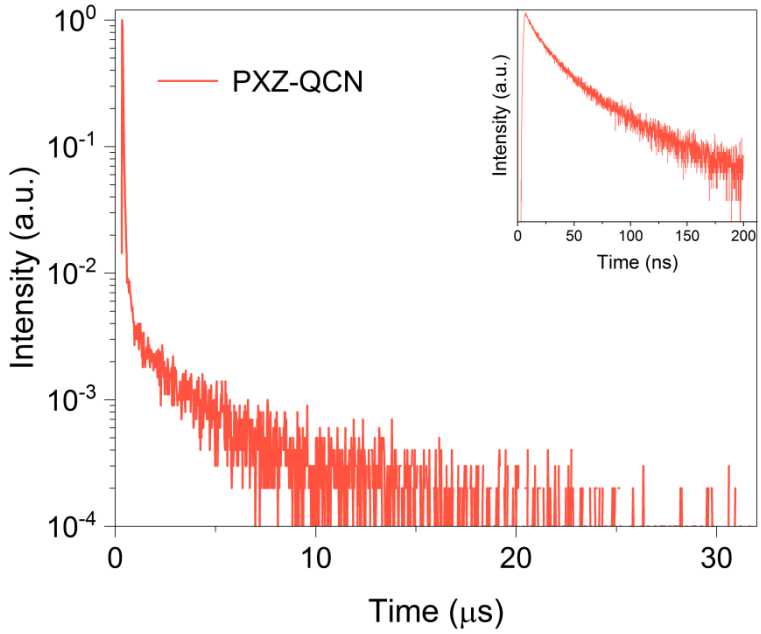

Figure S11. Transient PL decay curve of PXZ-QCN in 20 wt% doped CBP film at 298K.

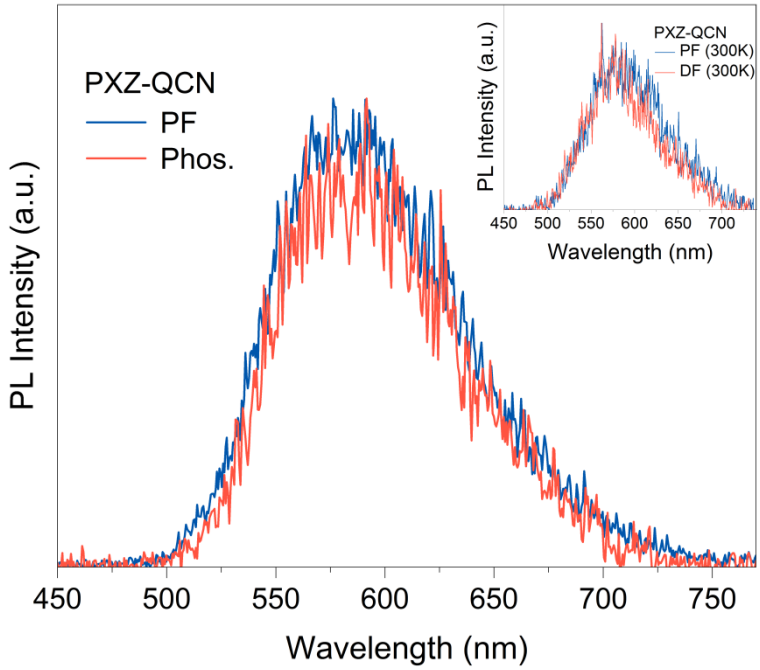

Figure S12. Time-resolved transient PL spectra of PXZ-QCN in 20 wt% doped CBP film at 77 K and 300 K (the inset).

Estimation for the Photophysical parameters

The quantum efficiencies and rate constants of the investigated compounds in 20 wt% CBP films are determined using the following equations S1-S6[2].

$$K_{PF} = \frac{1}{\tau_{PF}} \quad \text{S1}$$

$$K_{DF} = \frac{1}{\tau_{DF}} \quad \text{S2}$$

$$K_r^s \approx \frac{K_{PF}K_{DF}}{K_{RISC}} \Phi_{PL} \quad \text{S3}$$

$$K_{nr}^s \approx \frac{K_{PF}K_{DF}}{K_{RISC}} (1-\Phi_{PL}) \quad \text{S4}$$

$$K_{ISC} = \frac{K_{PF}K_{DF}\Phi_{DF}}{K_{RISC}\Phi_{PF}} \quad \text{S5}$$

$$K_{RISC} = \frac{K_{PF}+K_{DF}}{2} - \sqrt{\left(\frac{K_{PF}+K_{DF}}{2}\right)^2 - K_{PF}K_{DF}\left(1+\frac{\Phi_{DF}}{\Phi_{PF}}\right)} \quad \text{S6}$$

6. Theoretical Calculations

Table S7. Calculated spin-orbit coupling (SOC) constants of DMAC-QCN and PXZ-QCN.

Energy Level		$\langle S_n\|\hat{H}_{SOC}\|T_n\rangle$ (cm^{-1})	
S_n	T_n	DMAC-QCN	PXZ-QCN
0	1	2.4607	1.6667
1	1	0.0849	0.0894
1	2	0.0574	0.1179
1	3	0.2689	0.7116
1	4	0. 6930	0.5751
1	5	0.8793	0.0300

7. Electroluminescent properties

Table S8. Efficiency roll-off of the representative red TADF-based OLEDs with emission peak from 600 to 630 nm at a luminance of 1000 cd/m^2.

Emitter	Molecular structure	λ_{EL}	EQE_{max}	Roll-Off	Ref.
PXZ-QCN	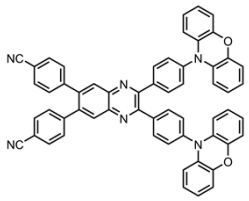	604	15.6	14.1	This work
PXZ-DCPP	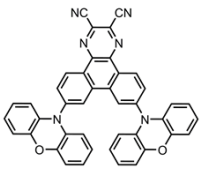	608	17.4	25.8	3
FDQPXZ	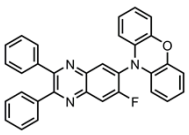	600	9.0	6.1	4
NZ2AC	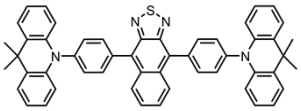	612	6.2	35.4	5

6AcBIQ	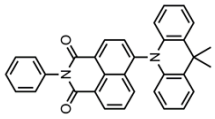	600	9.5	64.2	6
DPXZ-BPPZ	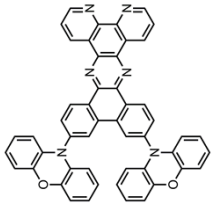	612	20.1	16.9	7
HAP-3TPA	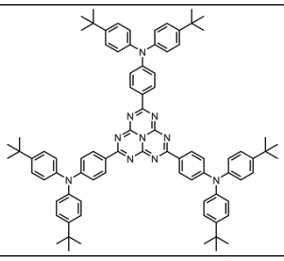	610	17.5	68.5	8
AQ-TPA	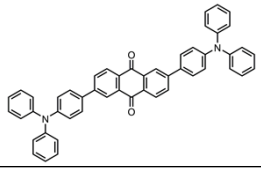	624	12.5	81.6	9
DPA-DCPP	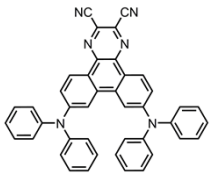	616	10.4	92.3	10
Bis-PXZ-PCN	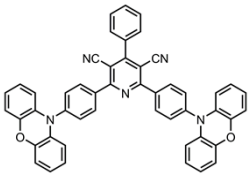	600	9.8	15.3	11
Tri-PXZ-PCN	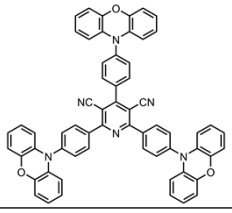	608	9.7	17.5	11
MeODP-DBPHZ	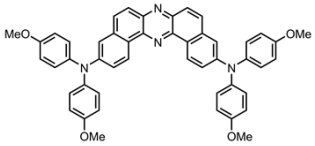	600	10.3	38.8	12

W1	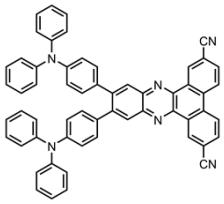	608	24.97	84.4	13
2PXZ-BP	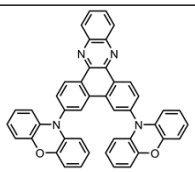	606	19.2	52.6	14
TPA–PZCN	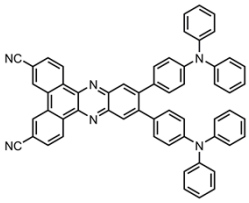	628	27.4	83.2	15
DPXZ-DPPM	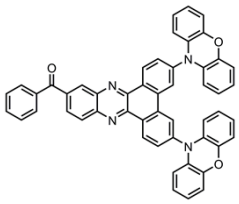	630	11.5	40.8	16
TAT−DBPZ	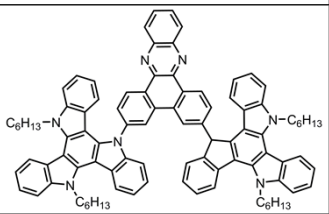	604	15.4	46.7	17
TAT−FDBPZ	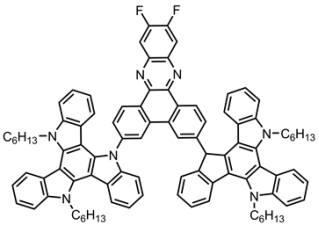	611	9.2	19.5	17
PQ2	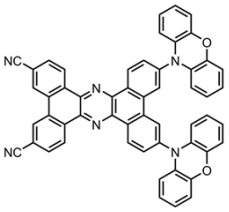	602	17.3	15.0	18
ANQDC-MSTA	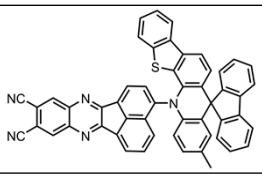	622	21.8	43.1	19

ANQDC-PSTA	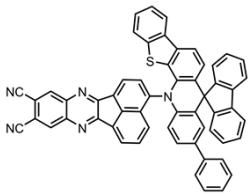	622	24.7	41.7	19
DPACNZP	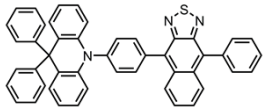	624	4.6	23.9	20
DTPAB	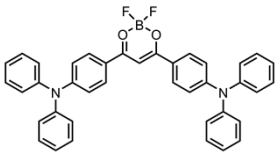	605	8.2	9.0	21
α-DMAC-DBP	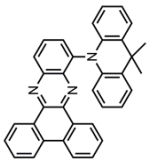	612	8.5	61.1	22
BDCN-PXZ	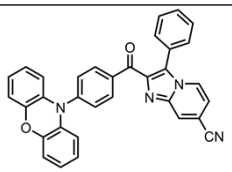	606	3.71	5.6	23

a) Estimated from the graphs in the references.

8. Reference

1. S.-C. Ji, T. Zhao, Z. Wei, L. Meng, X.-D. Tao, M. Yang, X.-L. Chen, C.-Z. Lu, *Chem. Eng. J*. 2022, **435**,134868.

2. Y. Wada, H. Nakagawa, S. Matsumoto, Y. Wakisaka, H. Kaji, *Nat. Photonics*, 2020, **14**, 643.

3. B. Wang, X. Qiao, Z. Yang, Y. Wang, S. Liu, D. Ma, Q. Wang, *Org. Electron*. 2018, **59**, 32-38.

4. L. Yu, Z. Wu, G. Xie, C. Zhong, Z. Zhu, H. Cong, D. Ma, C. Yang, *Chem Commun*. 2016, **52**, 11012-5.

5. T. Liu, L. Zhu, S. Gong, C. Zhong, G. Xie, E. Mao, J. Fang, D. Ma, C. Yang, *Adv. Opt. Mater*. 2017, **5**, 1700145.

6. J.H. Yun, J.Y. Lee, *Dyes. Pigm*. 2017, **144**, 212-217.

7. J.X. Chen, K. Wang, C.J. Zheng, M. Zhang, Y.Z. Shi, S.L. Tao, H. Lin, W. Liu, W.W. Tao, X.M. Ou, X.H. Zhang, *Adv. Sci*. 2018, **5**, 1800436.

8. J. Li, T. Nakagawa, J. MacDonald, Q. Zhang, H. Nomura, H. Miyazaki, C. Adachi, *Adv. Mater*. 2013, **25**, 3319-23.

9. Q. Zhang, H. Kuwabara, W.J. Potscavage, S. Huang, Y. Hatae, T. Shibata, C. Adachi, *J. Am. Chem. Soc*. 2014, **136**, 18070-81.

10. S. Wang, Z. Cheng, X. Song, X. Yan, K. Ye, Y. Liu, G. Yang, Y. Wang, *ACS*

Appl. Mater. Interfaces. 2017, **9**, 9892-9901.

11. Z. Chen, Z. Wu, F. Ni, C. Zhong, W. Zeng, D. Wei, K. An, D. Ma, C. Yang, *J. Mater. Chem. C*. 2018, **6**, 6543-6548.

12. P. Data, P. Pander, M. Okazaki, Y. Takeda, S. Minakata, A.P. Monkman, *Angew. Chem. Int. Ed*. 2016, **55**, 5739-44.

13. Y.-Y. Wang, Y.-L. Zhang, K. Tong, L. Ding, J. Fan, L.-S. Liao, *J. Mater. Chem. C*. 2019, **7**, 15301-15307.

14. F.M. Xie, P. Wu, S.J. Zou, Y.Q. Li, T. Cheng, M. Xie, J.X. Tang, X. Zhao, *Adv. Electron. Mater*. 2019, **6**, 1900843.

15. Y.L. Zhang, Q. Ran, Q. Wang, Y. Liu, C. Hanisch, S. Reineke, J. Fan, L.S. Liao, *Adv. Mater*. 2019, **31**, e1902368.

16. J. Liang, C. Li, Y. Cui, Z. Li, J. Wang, Y. Wang, *J. Mater. Chem. C*. 2020, **8**, 1614-1622.

17. Y. Liu, Y. Chen, H. Li, S. Wang, X. Wu, H. Tong, L. Wang, *ACS Appl. Mater. Interfaces*. 2020, **12**, 30652-30658.

18. U. Balijapalli, Y.T. Lee, B.S.B. Karunathilaka, G. Tumen-Ulzii, M. Auffray, Y. Tsuchiya, H. Nakanotani, C. Adachi, *Angew Chem. Int. Ed*. 2021, **60**, 19364-19373.

19. T. Hua, Y.-C. Liu., C.-W. Huang, Ne. Li, C. Zhou, Z. Huang, X. Cao, C.-C. Wu, C. Yang, *Chem. Eng. J*. 2022, **433**, 133598.

20. X. He, L. Gao, H. Liu, F. Liu, D. Jiang, C. Du, C. Sun, P. Lu, *Chem. Eng. J*. 2021, **404**, 127055.

21. J. Jin, W. Wang, P. Xue, Q. Yang, H. Jiang, Y. Tao, C. Zheng, G. Xie, W. Huang, R. Chen, *J. Mater. Chem. C*. 2021, **9**, 2291-2297.

22. J.H. Maeng, R. Braveenth, Y.H. Jung, S.J. Hwang, H. Lee, H.L. Min, J.Y. Kim, C.W. Han, J.H. Kwon, *Dyes. Pigm*. 2021, **194**, 109580.

23. Z. Qiu, W. Xie, Z. Yang, J.-H. Tan, Z. Yuan, L. Xing, S.Ji, W.-C. Chen, Y. Huo, S.-j. Su, *Chem. Eng. J*. 2021**, 415**, 128949.